HIGH RESOLUTION, MRI-BASED, SEGMENTED, COMPUTERIZED HEAD PHANTOM.

I. George Zubal, Charles R. Harrell, Eileen O. Smith, Amy L. Smith, Paul Krischlunas, Image Processing Group, Dept. of Diagnostic Radiology,
Yale University, New Haven, CT, 06510 USA

ABSTRACT

Purpose: We have created a high resolution software phantom of the human brain which is applicable to voxel-based radiation transport calculations yielding nuclear medicine simulated images and/or internal dose estimates.

Results: A software head phantom was created from 124 transverse MRI images of a healthy normal. The transverse T2 slices, recorded in a 256x256 matrix from a GE Signa 2 scanner, have isotropic voxel dimensions of 1.5 mm and were manually segmented by our clinical staff. Each voxel of the phantom contains one of 62 index numbers designating anatomical, neurological, and taxonomical structures. The result is stored as a 256x256x128 byte array. Internal volumes compare favorably to those described in the ICRP Reference Man.

Conclusion: The computerized array represents a high resolution model of a typical human brain and serves as a voxel-based anthropomorphic head phantom suitable for computer based modeling and simulation calculations. It offers an improved realism over previous mathematically described software brain phantoms, and creates a reference standard for comparing results of newly emerging voxel-based computations. Such voxel-based computations lead the way to developing diagnostic and dosimetry calculations which can utilize patient specific diagnostic images. However, such individualized approaches lack fast, automatic segmentation schemes for routine use; therefore, our high resolution, typical head geometry gives the most realistic patient model currently available.

INTRODUCTION

Computerized software phantoms serve an important role in simulating radiation transport geometries representing either therapeutic or diagnostic conditions. Much can be learned about the instrument characteristics, expected dose to human subjects, and anticipated image quality by computing such models on modern day computers. Several computer based phantoms have been developed over the last two decades in order to approximate the volume and orientation of internal organs of the human body (1-4). These have been, and are being used, to estimate the dose distribution in humans from external and internal radiation sources, or to evaluate imaging characteristics of radiological instruments. Broadly, these phantoms describe the surfaces or volumes of internal organs by two different methods: analytical equations describing the internal surfaces, or three dimensional arrays in which each voxel contains an index number assigning it to an organ.

The advantage of analytical descriptions is that they can very compactly store the surface information and allow one to very quickly compute the intersection of direction vectors with these surfaces. Their disadvantage lies in their inability to easily describe complicated, nonsmooth realistic structures within the human body. Voxel based phantoms can easily describe

complicated, convoluted surfaces by increasing the resolution of the array and appropriately assigning index numbers to the voxels. The disadvantage to voxel models is primarily two-fold: as the resolution of the arrays becomes higher, storage considerations become substantial; and, computing intersections of direction vectors with surfaces requires a voxel by voxel search.

Due in part to the recent interest in brain imaging, software phantoms which realistically model the human head are being developed and improved. We have developed a voxel based head phantom by manually drawing contours on 124 transverse MRI images of a healthy male volunteer.

This manual segmentation has resulted in a 256x256x128 byte array describing 62 anatomical, neurological, and taxonomical structures.

METHODS

We selected a volumetric MRI imaging sequence of a 35 year old male weighing 170 lbs and measuring 5' 10" in height, who was considered to be clinical normal and had no head abnormalities. The images were acquired on a GE Signa 1.5 Tesla scanner using SPGR mode ("spoiled grass"). These acquisitions are generally faster than spin echo sequences and demonstrate better gray to white ratios in the brain. Flow compensation was additionally implemented in order to eliminate any artifacts due to moving blood. The acquisition data was stored into a 256x192 matrix size which then is interpolated to 256x256 for carrying out the Fourier transform for image formation. With a field of view equal to 28 centimeters, the pixel size in the x, y, plane equals 1.1 mm. The resolution in the z axis results in a slice thickness of 1.4 mm. The single experiment (nex) acquisition time was 16 minutes.

The data access and processing programs were created on a VAX 3500 workstation running VMS version 5.0-2 using the available User Interface Services (UIS routines) for program control of the resident color display screen. The color display monitor is a 1024x1024 pixel raster display equipped with 8 bit planes. One bit plane is used for overlay graphics while the remaining 7 bits are used for mapping 128 color levels to the displayed transverse images. A serial line high resolution Summagraphics bitpad provided high resolution cursor control. An in-house program was developed to read the transverse slices from disk, display them on the color workstation monitor, and permit outlining of organs under bitpad cursor control. The x and y integer positions of all of the organ outlines are stored on disk with a resolution of 256x256 pixels. Members of the medical staff outlined separate internal organs and known structures contained in the transverse slices. A region of interest coloring routine was used to fill the inside of each organ outline with a unique index value. The MRI original slices were retained so that the original image matrix values can retrieved.

The segmented image information is stored in two independent files. A variable size file is created for each transverse slice and contains the x,y coordinates of each of the contours drawn on that slice. The slice number is retained in the name of the file. These contours serve as the input to the filling routine, which creates a fixed size organ index image. The organ index image is a 256x256 byte matrix filled with integer values which delineate the internal structures (organs) of the body. The organ index image is therefore, in effect, the original MRI T2 values, replaced by integers corresponding to the organ index value. The assignment of integers to the organs are shown in Table 1.

Table 1: Index numbers and their associated structures in the MRI images

0 outside phantom	77 cerebellum	105 putamen
1 skin	78 tongue	106 optic nerve
2 cerebral fluid	81 horn of mandible	107 internal capsule
3 spinal cord	82 nasal septum	108 septum pellucidium
4 skull	83 white matter	109 thalamus
5 spine	84 superior sagittal sinus	110 eyeball
9 skeletal muscle	85 medulla oblongata	111 corpus collosum
15 pharynx	88 artificial lesion	112 special frontal lobes
16 esophagus	89 frontal lobes	113 cerebral falx
22 fat	91 pons	114 temporal lobes
23 blood pool	92 third ventricle	115 fourth ventricle
26 bone marrow	95 occipital lobes	116 frontal portion eyes
29 trachea	96 hippocampus	117 parietal lobes
30 cartilage	97 pituitary gland	118 amygdala
63 lesion	98 fat	119 eye
70 dens of axis	99 uncus(ear bones)	120 globus pallidus
71 jaw bone	100 turbinates	121 lens
72 parotid gland	101 caudate nucleus	122 cerebral aquaduct
74 lacrimal glands	102 zygoma	123 lateral ventricles
75 spinal canal	103 insula cortex	124 prefrontal lobes
76 hard palate	104 sinuses/mouth cavity	125 teeth

RESULTS

In order to appreciate the internal detail of the voxel based head phantom, we present three selected transverse slices from the segmented volume array in Figure 1.

Another way to appreciate the volumetric structures in our phantom is to fill selected structures with positive integer values and leave other structures filled with zero. Then the three dimensional volume can be collapsed along each of the three axes in order to obtain a two dimensional representation of the original three dimensional volume. Since the volume is collapsed by adding the integers filled into the voxels, each of the three views corresponds to a projection of the volume onto a plane. Several internal structures were selected and filled with integer values in order to highlight the skull, white matter, caudate nucleus, putamen, thalamus, globus pallidus, and eye. These are shown in Figures 2 and 3.

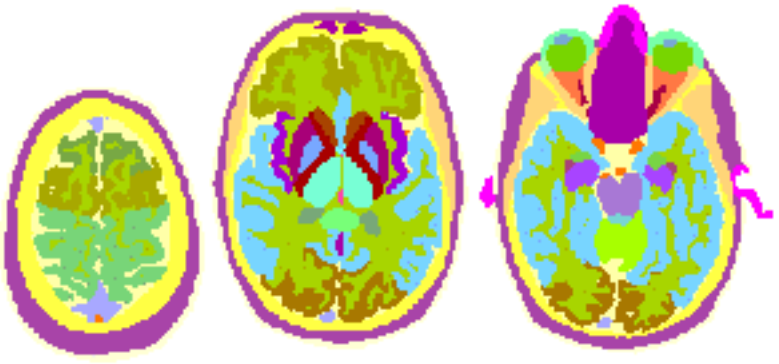

Figure 1: Three arbitrarily selected transverse slices from the segmented phantom volume. The gray level used to display each structure is directly related to the index number in Table 1.

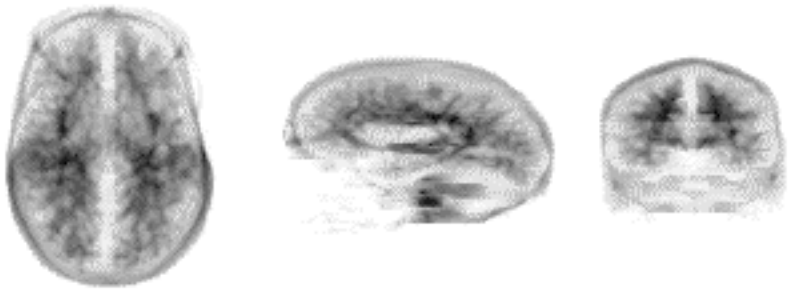

Figure 2: A vertex, lateral, and anterior view of the phantom with opacity filled into all voxels corresponding to white matter and skull.

Figure 3: A vertex, lateral and anterior view of the phantom with opacity filled into all voxels corresponding to skull, caudate nucleus, putamen thalamus, globus pallidus, and eye (excluding the lens).

Since the volume (or weight) of each structure is important for both therapeutic and diagnostic applications, we determined the number of voxels contained in each structure and by knowing the voxel dimensions, calculated the structure sizes (see Table 2).

Table 2: List of the segmented internal structures and their associated volume in cubic centimenters.

skin	236.7	cerebellum	139.4	putamen	10.3
cerebral fluid	220.6	tongue	17.6	optic nerve	1.5
spinal cord	2.9	horn of mandible	14.9	internal capsule	9.2
skull	459.9	nasal septum	5.7	septum pellucidium	0.9
spine	26.8	white matter	510.7	thalamus	12.3
skeletal muscle	361.3	super.sagittal sinus	4.1	eyeball	12.9
pharynx	4.5	medulla oblongata	3.9	corpus collosum	10.9
esophagus	-	artificial lesion	4.7	sp. reg. fr. lobes	6.56
fat	52.6	frontal lobes	112.8	cerebral falx	4.50
blood pool	24.3	pons	22.4	temporal lobes	231.1
bone marrow	0.9	third ventricle	8.9	fourth ventricle	1.9
trachea	-	occipital lobes	70.1	fr. portion eyes	5.2
cartilage	51.1	hippocampus	7.1	parietal lobes	120.1
lesion	-	pituitary gland	0.086	amygdala	3.9
dens of axis	1.3	fat	501.1	eye	13.4
jaw bone	5.54	uncus(ear bones)	0.8	globus pallidus	4.1
parotid gland	31.3	turbinates	6.4	lens	0.48
lacrimal glands	2.5	caudate nucleus	10.5	cerebral aquaduct	0.5
spinal canal	7.7	zygoma	9.4	lateral ventricles	9.5
hard palate	30.3	insula cortex	13.1	prefrontal lobes	53.2
		sinuses/mouth	172.6		

Four of the structures found in Table 2 were listed in the ICRP Reference Man Report (5): cerebellum = 143 grams, thalamus = 6.5 grams, eye ball = 13.5 grams, lens of the eye = .4 grams. Except for the thalamus the volume determinations for this one individual are virtually identical to those documented in the Reference Man Report. It is not clear to us why the thalamus in this individual is approximately twice that sited in the literature.

Data Archive: Three data sets have been stored.

1. The raw MRI data files are stored in a 256x256 two-byte signed integer array. Depending upon hardware, the bytes of these words may need to be swapped before displaying.
2. Segmented image data in a 256x256 one-byte array. Each byte represents a pixel continuing an index number to an associated internal structure. Slice 1 starts at the roof of mouth and slice 124 ends at the top of the head.
3. The x,y contours which were manually drawn to segment the internal structures are saved as a list of x,y pairs.

The total storage capacity of the files are: original MRI images = 36 Megabytes, organ index matrices = 28 Megabytes , x,y contours = 3 Megabytes, and are available for public access through our Imaging Processing and Analysis Laboratory. To gain access to the data, send a request to Dr. George Zubal e-mail: George.Zubal@Yale.Edu.

ACKNOWLEDGMENTS

Work performed under contract #DE FG02-88ER60724 with the US Department of Energy and under contract #NS32879 with the US National Institutes of Health. We are thankful to Vivian Ventura for her text processing skills.

REFERENCES

(1) Snyder, W, Ford, MR, Warner, G :"Estimates of Specific Absorbed Fractions for Photon Sources Uniformly Distributed in Various Organs of a Heterogeneous phantom". NM/MIRD Pamphlet No. 5.,Society of Nuclear Medicine Publication., New York, (1978).

(2) Williams, G, Zankl, M, Abmayr, W, Veit, R, Drexler, G: "The Calculation of Dose from External Photon Exposures using Reference and Realistic Human Phantoms and Monte Carlo Methods", Phys. Med. Bio.,**31**, 449-452, (1986).

(3) Wang, H, Jaszczak, RJ, Coleman, RE: "Solid Geometry-Based Object Model for Monte Carlo Simulated Emission and Transmission Tomographic Imaging Systems." IEEE Transactions on Medical Imaging, **11**, 361-372, (1992).

(4) Zubal IG, Harrell CR, Smith EO, Rattner Z, Gindi G, Hoffer PB. "Computerized 3-Dimensional Segmented Human Anatomy", Medical Physics, 21(2), February 1994, p. 299-302 .

(5) Snyder WS, Cook MJ, Masset ES, Kaehausen LR, Howells GP Tipton IH, ICRP No23 Report of the Task Group on Refernce Man, Pergamon Press (1984).